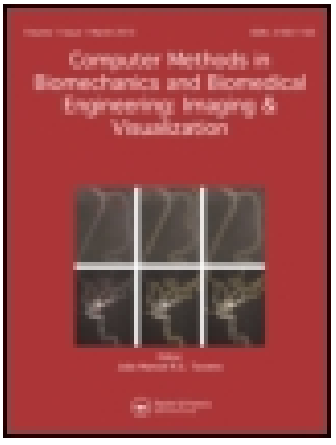

Computer Methods in Biomechanics and Biomedical Engineering: Imaging & Visualization

Publication details, including instructions for authors and subscription information:
http://www.tandfonline.com/loi/tciv20

New estimation method of the contrast parameter for the Perona-Malik diffusion equation

M. Borroto-Fernández[a], M. González-Hidalgo[b] & A. León-Mecías[a]

[a] Facultad de Matemática y Computación, Universidad de la Habana, San Lázaro y L, Habana 4 CP-10400, Cuba

[b] Department of Mathematics and Computer Science, University of the Balearic Islands, E-07122 Palma de Mallorca, Spain

Published online: 29 Oct 2014.

To cite this article: M. Borroto-Fernández, M. González-Hidalgo & A. León-Mecías (2014): New estimation method of the contrast parameter for the Perona-Malik diffusion equation, Computer Methods in Biomechanics and Biomedical Engineering: Imaging & Visualization, DOI: 10.1080/21681163.2014.974289

To link to this article: http://dx.doi.org/10.1080/21681163.2014.974289

Computer Methods in Biomechanics and Biomedical Engineering: Imaging & Visualization, 2014
http://dx.doi.org/10.1080/21681163.2014.974289

New estimation method of the contrast parameter for the Perona–Malik diffusion equation

M. Borroto-Fernández[a], M. González-Hidalgo[b] and A. León-Mecías[a]*

[a]*Facultad de Matemática y Computación, Universidad de la Habana, San Lázaro y L, Habana 4 CP-10400, Cuba;* [b]*Department of Mathematics and Computer Science, University of the Balearic Islands, E-07122 Palma de Mallorca, Spain*

(*Received 31 January 2014; accepted 5 October 2014*)

The aim of this contribution is to make an efficient smoothing algorithm that preserves edges and provides valuable information for any segmentation process. The non-linear anisotropic diffusion (AD) model of Perona–Malik is considered to enhance the edges in the process of diffusion through a variable diffusion coefficient. However, the diffusion coefficient is very sensitive to the so-called contrast or gradient threshold parameter. This article proposes a novel methodology for the estimation of this contrast parameter based on a partition of the image using the *K*-means algorithm and a least-square fit to approximate the diffusion coefficient (KMLS). The experimental results show that the quality of the edge detection process improves when the proposed algorithm in the smoothing AD is used instead of the traditional techniques. The comparison is performed using two objective edge detection performance measures, the so-called Pratt's figure of merit and the symmetric average distance. Both measures show great improvements if we use the Perona–Malik equation with the KMLS estimator.

Keywords: contrast parameter; objective performance measures; anisotropic diffusion; Perona–Malik equation; K-means algorithm; KMLS estimator

1. Introduction

The use of digital images as a valuable instrument to store and process information reaches an amazing diversity of research fields such as medical applications, computer graphics, computer vision, applications in meteorology and telecommunications, among others. Image processing is then an interesting current study field. We focus our interest on a processing task which frequently arises from numerous applications: image smoothing. Image smoothing has a significant role in image preprocessing in order to produce an image with much higher quality, to enhance its sharpness, to filter out the noise, or simply to prepare the image for a forthcoming analysis. Image smoothing is particularly important as a previous step for edge detection and image segmentation. For enhancing different features, different techniques have been used: linear and non-linear filtering for denoising and restoration (Chan and Shen 2005; Bankman 2008; Bovik 2009), wavelets-based methods (Chan and Shen 2005; Mallat 2008; Bovik 2009) and partial differential equation (PDE)-based method (Perona and Malik 1990; Weickert 1998; Chan et al. 2003; Weeratunga and Kamath 2003; Chan and Shen 2005) among others.

In this work, we are interested in image smoothing that keeps edges, considering that edge enhancement in images has great importance because the human visual system uses edges as a key factor in the comprehension of the contents of an image (Bankman 2008). Among the image smoothing PDE-based methods, Perona and Malik (1990) proposed for the first time a non-linear diffusion based algorithm that overcame the disadvantages of the linear diffusion such as blurring or dislocating the edges of the image. Perona and Malik recognised the importance of the scale-space representation of an image, which was introduced by Witkin (1983), and later developed by Koenderink (1984). In Koenderink (1984), the evolution of an image under Gaussian scale-space (which is obtained via convolution with Gaussians of increasing variance or equivalently by linear diffusion filtering) is used to make a deep structure analysis for extracting semantic information from an image. A disadvantage of Gaussian smoothing is the fact that it does not only smooth the noise, but also blurs important features such as edges and thus, it makes them difficult to identify. However, linear diffusion filtering dislocates edges when moving from finer to coarser scales, Witkin (1983). Then, there is a need to establish an agreement between noise elimination and preserving the image structure. To this end in Perona and Malik (1990) the diffusion process modelled by a non-linear PDE with variable diffusion coefficient is considered, specifically the diffusion coefficient c is chosen as an appropriate function of the gradient of the brightness function, $c(x, y, t) = g(\|\nabla I(x, y, t)\|)$.

The Perona–Malik model has been widely used in image processing for purposes such as smoothing, restoration, segmentation, filtering or detecting edges; specifically in biomedical imaging you can see Mendrik et al. (2009) and Chai et al. (2011). Several practical, and

*Corresponding author. Email: angela@matcom.uh.cu

theoretical difficulties of this model have been avoided using for instance regularising methods (Alvarez et al. 1992; Catté et al. 1992; Weickert 1998). Different methods have been suggested for the discretisation of the non-linear operator and the numerical solution of the PDE (Kaur and Mikula 1995; Weickert 1998; Weickert et al. 1998; Barash and Kimmel 2000; Duarte-Carvajalino et al. 2007; Zhang and Yang 2010; Chen et al. 2011). To achieve a better performance in edge preserving, different expressions for the diffusion coefficient have been proposed (Perona and Malik 1990; Charbonnier et al. 1997; Black et al. 1998; Weickert 1998; Gilboa et al. 2002). All the given expressions depend on a parameter k in such a way that in those region of the image where $\|\nabla I\| > k$, the smoothing effect is weaker and then the edges are preserved and where $\|\nabla I\| < k$ the smoothing effect is stronger. It means that k is a contrast parameter or a threshold for the magnitude of the gradient of the brightness with a great influence in edge preserving. It is evident that the diffusion coefficient is very sensitive to the choice of the parameter k. At the same time, k has to be chosen taking into account local changes of the brightness gradient. However, regarding this parameter k that in one way or another interferes with the diffusion process, very few works have been written.

The goal of this work is to obtain a general methodology to estimate this contrast parameter k for grey-scale images. The K-means algorithm and a least-square fit are used to approximate the diffusion coefficient (KMLS). A specific expression for the diffusion coefficient is used to show how to obtain k. Examples demonstrate that preprocessing by the anisotropic diffusion (AD) model of Perona–Malik, when KMLS is used instead traditional methods, improves significantly a subsequently edge detection.

This work is organised as follows: in Section 2, we present some elements about AD including different expressions for the diffusion coefficient, containing all of them the so-called contrast parameter k. In Section 3, we discuss the importance of the right choice of the contrast parameter in the diffusion coefficient and we present a novel algorithm to select it. In Section 4, we show that adding our algorithm to the Perona–Malik equation, the subsequently edge detection improves considerably. For the discussion of results, two objective performance measures on edge detection are used. Some remarks are presented in Section 5.

2. Image smoothing by diffusion

The simplest way to smooth an image is to apply a Gaussian filter $G_\sigma(x,y) = (1/2\pi\sigma^2)\mathrm{e}^{-(x^2+y^2)/2\sigma^2}$ of successively larger σ values. The resulting sequence of images builds a Gaussian scale-space, where each scaled image is calculated by convolving the original image with a Gaussian filter of increasing σ value. As σ is increased, less significant image features and noise begin to disappear, leaving only large-scale image features. It is well known (Koenderink 1984; Weickert 1998) that the Gaussian scale-space may also be viewed as the evolving solution of a PDE $(\partial I(x,y,t))/\partial t = c\Delta I(x,y,t)$. The time–scale relationship is defined by $\sigma = q\sqrt{t}$. However, the linear diffusion equation not only removes noise but also blurs the image (Weickert 1998), specifically by constant diffusion coefficient c, all locations in the image including the edges are equally smoothed. Due to the valuable information we can get from image edges, we are interested in the non-linear diffusion model proposed in Perona and Malik (1990). In order to avoid image blurring and localisation difficulties of linear diffusion filtering, and to be able to control the diffusion near the edges, the Perona–Malik model consists of a non-linear PDE that uses an inhomogeneous diffusion coefficient,

$$\frac{\partial I(x,y,t)}{\partial t} = \mathrm{div}(c(x,y,t)\nabla I(x,y,t)), \quad \text{in } \Omega \times (0,T), \tag{1a}$$

$$c(x,y,t)\nabla I(x,y,t)\cdot N = 0, \quad \text{in } \partial\Omega \times (0,T), \tag{1b}$$

$$I(x,y,0) = I_0(x,y), \quad \text{in } \Omega, \tag{1c}$$

where $\Omega \subset \mathbb{R}^2$, $I(x,\ y,\ 0)$ is the original image intensity function and $I(x,\ y,\ t)$ is the smoothed image intensity function in time t. The diffusion coefficient c is chosen as $c(x,y,t) = g(\|\nabla I(x,y,t)\|)$. Although the Perona–Malik model is called of AD in the field of differential equations, this term is used when the diffusion coefficient c is a tensor, see Weickert (1999). We consider c as a function depending on time and space.

2.1 The diffusion coefficient: control instrument to preserve edges

In the literature several expressions for the diffusion coefficient can be found. In Table 1, some of them are shown.

This coefficient, as the name suggests, characterises the diffusion process in the medium where it is taking place; for a constant coefficient, the diffusion process is carried out in equal measure over all the region. However, if this is variable, it means that if it depends on time and position, the diffusion is performed wholly different across the medium and that is precisely used by Perona and Malik when defining $g_1(s)$ and $g_2(s)$ in Table 1 ($g_4(s)$ is only a little modification of $g_1(s)$ which has a more stable character according to Voci et al. (2004)). In Perona and Malik (1990), these expressions were defined in a way that would lead smoothing within each region on the image bounded by the edges and not across the boundaries. During the diffusion process the image is iteratively

Table 1. More used expressions for the diffusivity function.

$g(s^2)$	References
$g_1(s) = \frac{1}{1+(s^2/k^2)}$	Perona and Malik (1990)
$g_2(s) = \exp\left(\frac{-s^2}{2k^2}\right)$	Perona and Malik (1990)
$g_3(s) = \begin{cases} \frac{1}{2}\left[1-\frac{s^2}{2k^2}\right]^2, & s \le \sqrt{2k} \\ 0, \text{ in other case} \end{cases}$	Tukey's biweight, Black et al. (1998)
$g_4(s) = \frac{1}{\sqrt{1+(s^2/k^2)}}$	Charbonnier et al. (1997)
$g_5(s) = \begin{cases} 1, & s \le 0 \\ 1-\exp(-C_m/(s/k)^m), & s > 0 \end{cases}$ $m = 2$, 3 and 4, $C_m = 2.33666$, 2.9183 and 3.31488	Weickert (1998)
$g_6(s) = \frac{1}{1+(s/k_f)^n} - \frac{\alpha}{1+((s-k_b)/\omega)^2 m}$	Gilboa et al. (2002)

modified according Equation (1(a)) and this way to pick the coefficient allow us to have control of the smoothing over the edges all the time. As the locations of the edges are not known in advance, an estimation of these is needed. A possible choice that indicates the presence of edges, as mentioned earlier, is the magnitude of the gradient of the intensity function that is, $s = \|\nabla I\|$ (see Table 1). AD, as was stated by Perona and Malik, removes noise from an image preserving the region boundaries. It means that the diffusion process will mainly take place in the interior of regions, and it does not affect the region boundaries where the magnitude of $\|\nabla I\|$ is large. This can be achieved taking as diffusion coefficient a function that depends on the magnitude of the image intensity gradient, $c(x, y, t) = g(\|\nabla I(x, y, t)\|)$, such that $g(\|\nabla I\|) \to 1$ for $\|\nabla I\| \to 0$, which means that the diffusion is maximal within uniform regions and $g(\|\nabla I\|) \to 0$ for $\|\nabla I\| \to \infty$ so that the diffusion is stopped across edges. In other words, this function should be monotonically decreasing so that the diffusion or the smoothing decreases as the gradient strength increases and the diffusion is stopped across edges. $\|\nabla I\|$ serves only as an edge detector, for more details see Perona and Malik (1990).

Besides the expressions $g_1(s)$ and $g_2(s)$ given by Perona and Malik, there are others, for instance in Black et al. (1998) the expression given by $g_3(s)$ was obtained using the equivalence between image smoothing by AD and its estimation from noisy data in the framework of robust statistics. Specifically, $g_3(s)$ was obtained by using a robust standard error estimation norm, the known Tukey's biweight. Smoothed versions where $(\nabla I)^2$ is replaced by a Gaussian convolution $G_\sigma * \nabla I$ are also used, see Catté et al. (1992) and Gilboa et al. (2002). $g_5(s)$ can be regarded as an anisotropic regularisation of the Perona–Malik model; the constant C_m is calculated in such a way that the flux $\phi = sg(s)$ is increasing for $s \in [0, k]$ and decreasing for $s \in (k, \infty)$. In Weickert (1998) the choice $m = 4$ gave visually good results. In order to overcome three major problems associated with the linear backward diffusion process, namely the explosive instability, noise amplification and oscillations, in Gilboa et al. (2002) a diffusion coefficient as $g_6(s)$ that assumes both positive and negative values is considered.

If we observe all the expressions for the diffusion coefficient that appear in Table 1, we can see that they have a common characteristic: all expressions are influenced by a parameter k. In image regions where $\|\nabla I\| > k$, the smoothing effect is less and the edges are preserved, and for $\|\nabla I\| < k$ the diffusion coefficient is larger and the smoothing effect is greater. In other words, k is a contrast parameter or gradient threshold. Figure 1 illustrates that the behaviour of the diffusion coefficient is sensitive to the choice of this contrast parameter. After the same number of iterations, the smoothing effect resulting from the diffusion process is different for different values of k. If we increase the value of k, the diffusion process blurs the image, removing the details, as is shown in Figure 1(d)).

Taking into account that during the diffusion the image is smoothed and with this the value of the gradient

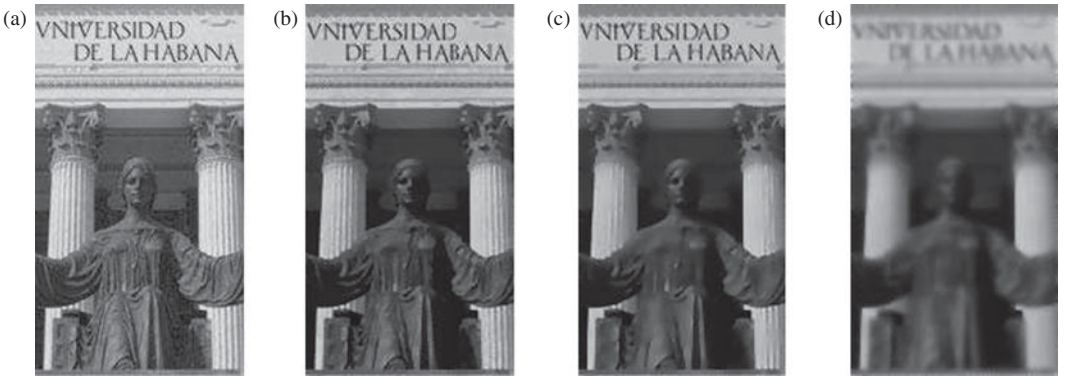

Figure 1. (a) Original image. (b)–(d) Smoothed images after 20 iterations with $k = 6$, 13 and 50, respectively.

decreases, then the value of the parameter k that controls the rate of the diffusion must also fall, so that the edges are preserved, $\|\nabla I\| > k$. Then k should depend on time. Therefore, it is mandatory that the parameter k is determined in an optimal way in every step of the iterative process, and finally the quality of the edges obtained for a given image is evaluated. The goal of this article is to address this topic.

3. Estimating the contrast parameter

In the literature, there are some ways to estimate the so-called contrast parameter, such as noise estimator proposed by Perona and Malik (1990) and described by Canny (1986), the morphological filtering and the p-norm estimator by Voci et al. (2004). The fundamental problem with these estimations is that the method depends on the images that have been used, so to use this in other pictures is not necessarily successful. In a recent work (Tsiotsios and Petrou 2013), the estimation of two gradient threshold parameters has been proposed, instead of one. These two parameters refer to the vertical and the horizontal directions for the discrete approximation of the gradient operator, which allow to write the discrete AD equation in a more precise way. Our proposal develops a methodology for the estimation of a contrast parameter or gradient threshold where any expression for the diffusion coefficient can be used.

3.1 *Partition and adjustment methodology*

We propose a new method to estimate the contrast parameter for grey level images, based on a methodology that we call 'Partition and Adjustment'. This methodology combines a clustering method and a curve fitting method. The clustering method is used to make a partition of the set P of pixels of the image according to its intensity gradient magnitude. Considering this partition and using a curve fitting method, with a specific expression for the diffusion coefficient, an appropriate value for the parameter k is obtained. The estimation of k is obtained for each time step, that is for each iteration of the differential equation. While the diffusion process is taking place, the values of intensity of the pixels are changing, then in order to obtain a new value of k for each time step, we have to perform the pixel partition again and the estimation of the diffusion coefficient. The goal is to preserve both strong edges and weak edges. Recall that the idea is that in the diffusion process the edges do not get lost, so we have to force the diffusion coefficient function to take values close to 0 for the pixels belonging to the edges and close to 1 for the pixels that do not belong to the edges.

The set P of pixels is partitioned into three subsets P_1, P_2 and P_3, where P_1 is the subset of pixels that does not belong to the edges of the image, P_3 is the subset of pixels belonging to the edges of the image and finally, P_2 is the subset of pixels called fuzzy set because its elements can be weak edges or cannot be edges, $P_2 = P\backslash(P_1 \cup P_3)$. Figure 2 illustrates schematically our proposal. It shows for any expression of the coefficient, the relationship between the behaviour required for the diffusion coefficient in the AD with the parameters that we have chosen for its estimate in each iteration step of the differential equation. As mentioned earlier, the diffusion coefficient $c(x, y, t)$ should be a monotonically decreasing function so that the diffusion or the smoothing decreases as the gradient strength increases and the diffusion is stopped across edges ($c(x, y, t) = g(\|\nabla I\|) \to 0$ for $\|\nabla I\| \to \infty$), as it can be seen in P_3. Figure 2 also shows that given the partition, the ideal thing would be to have a strong smoothing in P_1, a weak smoothing in P_3 and a half term

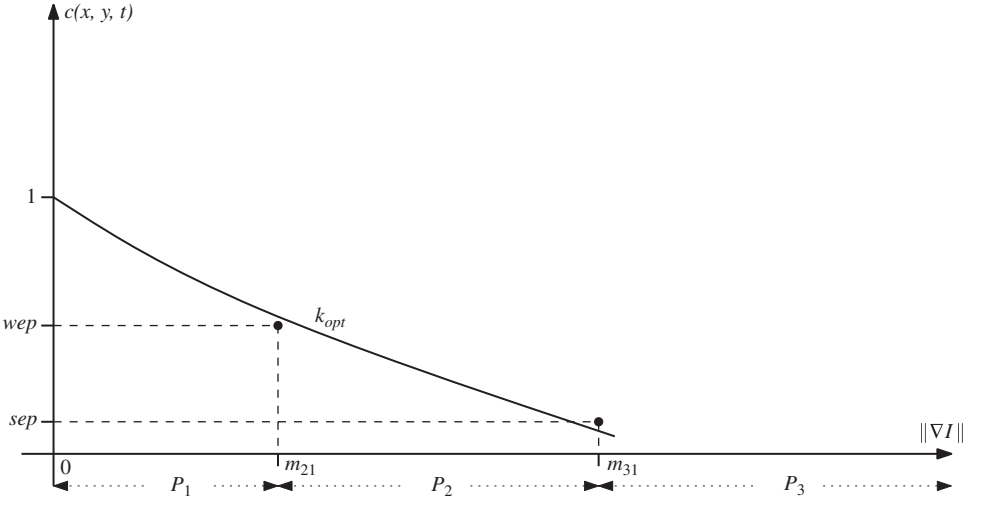

Figure 2. Illustration of partition and adjustment methodology.

smoothing in P_2, controlled by a threshold that preserves the details. To achieve this goal, given the partition, two important values are defined, m_{21} and m_{31}, as the lower values of the gradient magnitude of the pixels in P_2 and P_3, respectively. At this point, the behaviour of the diffusion coefficient depends on the properties of the treated image in the sense that the values of the intensities of the magnitude of the gradient are not the same ones and therefore a different partition exists for each image, then we have different values for m_{21} and m_{31}.

In addition, to control the intensity of the smoothing process over the different subsets, two thresholds are defined: weak edge preserving (*wep*) and strong edge preserving (*sep*). These two thresholds are values that the diffusion coefficient will take for two values of the magnitude of the gradient. It means we have the following constraints for the diffusion coefficient function in each fixed time step $t = \tilde{t}$.

$$c(x, y, \tilde{t}) \leq sep, \quad (x, y) \in P_3, \tag{2}$$

$$sep < c(x, y, \tilde{t}) < wep, \quad (x, y) \in P_2, \tag{3}$$

$$c(x, y, \tilde{t}) \geq wep, \quad (x, y) \in P_1. \tag{4}$$

The *sep* should be in a zero neighbourhood, because the diffusion process should preserve the subset of pixels of P_3 since they belong to the strong edges of the image, which means that the diffusion coefficient should converge to 0 for the pixels in P_3.

In addition, the selection of the threshold of preservation of weak edges *wep* requires information of the image because it depends on the smallest value of intensity considered for the pixels of weak edges in P_2. The diffusion coefficient will take the value *wep* when the magnitude of the gradient is equal to m_{21}, which is in turn in the frontier of the pixels that are not considered as edge and where we want to have a half term smoothing. Considering that the diffusion coefficient takes values between 0 (not diffusion) and 1 (maximal diffusion), and in order to strongly smooth the pixels in P_1 without involving the pixels in P_2, the threshold *wep* should be in a neighbourhood of 0.5 to have half term smoothing. We have obtained very good experimental results taking $wep = 0.5$. As you can see in Figure 3, varying the threshold *wep* and keeping *sep* equal to 0.01 the diffusion of a panther image is carried out and the corresponding edge images are displayed. If one looks more carefully the difference is appreciated, for instance, in the ear of the panther.

In addition, the threshold *sep* takes values close to zero because this value belongs together with the diffusion intensity for the pixels that have the smallest value of intensity considered in P_3 and these should be preserved (they should not be smoothed) as it can be seen in Figure 2. Therefore, the contrast parameter k should be such that the diffusion coefficient $c(x, y, t)$ is close to zero. In Figure 4, varying the threshold *sep* and keeping *wep* equal 0.5 the diffusion of a panther image is carried out and also the corresponding edge images are displayed. It is observed that as the value of the threshold *sep* grows more edges are eliminated. In view of the previously described and in the experimental results, a reasonable combination for our coefficients is with $sep = 0.01$ and $wep = 0.5$.

The previous discussion and the experiments show that the best combination is with $sep = 0.01$ and $wep = 0.5$.

3.2 KMLS estimator

In this section, our estimator for the contrast parameter is introduced. We call it KMLS estimator because of the K-means clustering method, see Duda et al. (2001) and the least square curve fitting, Stoer and Bulirsch (1993). We have chosen K-means because it is very simple to implement and we know the number of clusters ($K = 3$). However, another clustering method can be used. For the approximation of the diffusion coefficient, the least squares method has been selected, but different types of curve fits can be used. Therefore, the proposed methodology generates a family of estimators. To illustrate the procedure, we estimate the contrast parameter for the coefficient expression g_2 given in Table 1.

Step 1: Apply K-means to get the partition $\{P_1, P_2, P_3\}$ of the set P of pixels of the image. The parameters of the K-means algorithm are as follows:

- Number of clusters
  $K = 3$.
- Initial means

$$\mu_1 = \min\{\|\nabla I\|_{(x,y)} : (x, y) \in P\} \quad \text{for } P_1, \tag{5a}$$

$$\mu_3 = \max\{\|\nabla I\|_{(x,y)} : (x, y) \in P\} \quad \text{for } P_3, \tag{5b}$$

$$\mu_2 = \frac{\mu_1 + \mu_3}{2} \quad \text{for } P_2. \tag{5c}$$

- Operations
  (a) Distance:

$$\mathrm{d}((x, y), \mu_i) = \left| \|\nabla I\|_{(x,y)} - \mu_i \right| \quad i = 1, 2, 3.$$

  (b) Add:

$$a((x_1, y_1), (x_2, y_2)) = \|\nabla I\|_{(x_1,y_1)} + \|\nabla I\|_{(x_2,y_2)}.$$

The gradient magnitude values m_{21} and m_{31} are selected.

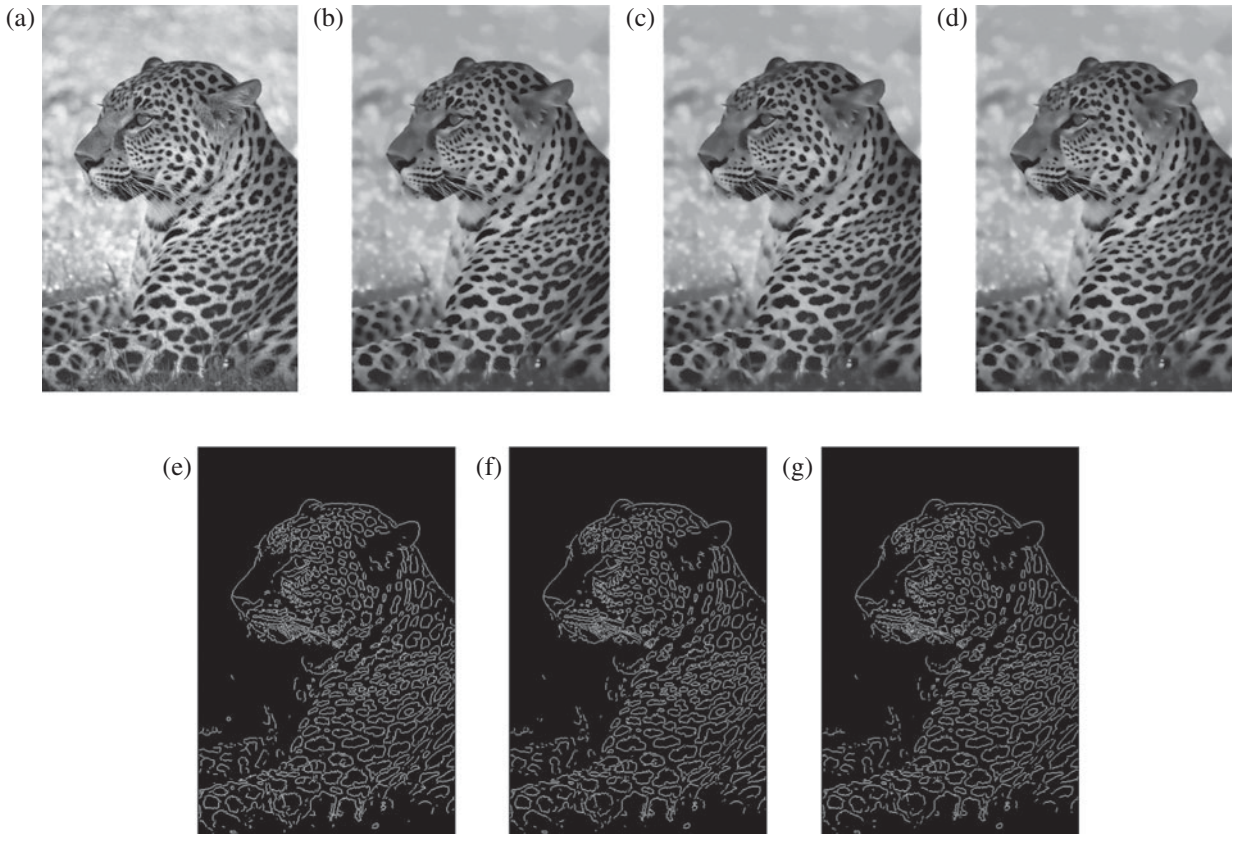

Figure 3. (a) Original panther image. (b)–(d) Smoothed versions of the image by AD with threshold $sep = 0.01$ and $wep = 0.2$, 0.5 and 0.9, respectively, to fit the diffusion coefficient. (e)–(g) The respective edge images.

Step 2: Make the least squares fitting of $c(x, y, t) = g_2(\|\nabla I(x, y)\|)$, with

$$g_2(\|\nabla I(x, y)\|) = \mathrm{e}^{-[\|\nabla I(x,y)\|/k]^2},$$

and the values given in Table 2.

Then, we define

$$S(k) = \left[sep - \mathrm{e}^{-(m_{21}^2/k^2)}\right]^2 + \left[wep - \mathrm{e}^{-(m_{31}^2/k^2)}\right]^2, \quad (6)$$

and solve the equation

$$\frac{\mathrm{d}S}{\mathrm{d}k} = 0. \quad (7)$$

Finally, we obtain the following expression for the contrast parameter k

$$k = \sqrt{-\frac{m_{21}^2 + m_{31}^2}{\ln(sep \times wep)}}. \quad (8)$$

The contrast parameter was estimated at each integration step $m\Delta t$ of the Perona–Malik equation, because it is a time variable function as the gradient of the image, which varies with the diffusion process. Finally, we have the next expression

$$k_{m\Delta t} = \sqrt{-\frac{m_{21_{m\Delta t}}^2 + m_{31_{m\Delta t}}^2}{\ln(sep_{m\Delta t} \times wep_{m\Delta t})}}. \quad (9)$$

It is relevant to highlight that the proposed methodology does not depend on a specific expression of the diffusion coefficient. However, for some expression, the solution of Equation (7) has an additional cost. For example, if we use the expression described by $g_1(s)$ in Table 1, Equation (7) becomes

$$c_8 k^8 + c_6 k^6 + c_4 k^4 + c_2 k^2 + c_0 = 0, \quad (10)$$

where

$$c_{2i} = f_i(m_{21}, m_{31}, sep, wep), \quad \text{for } i = 0, 1, 2, 3, 4.$$

In this case, it is impossible to obtain an explicit expression for k. Then, it is necessary to use a numerical method such as the Newton method.

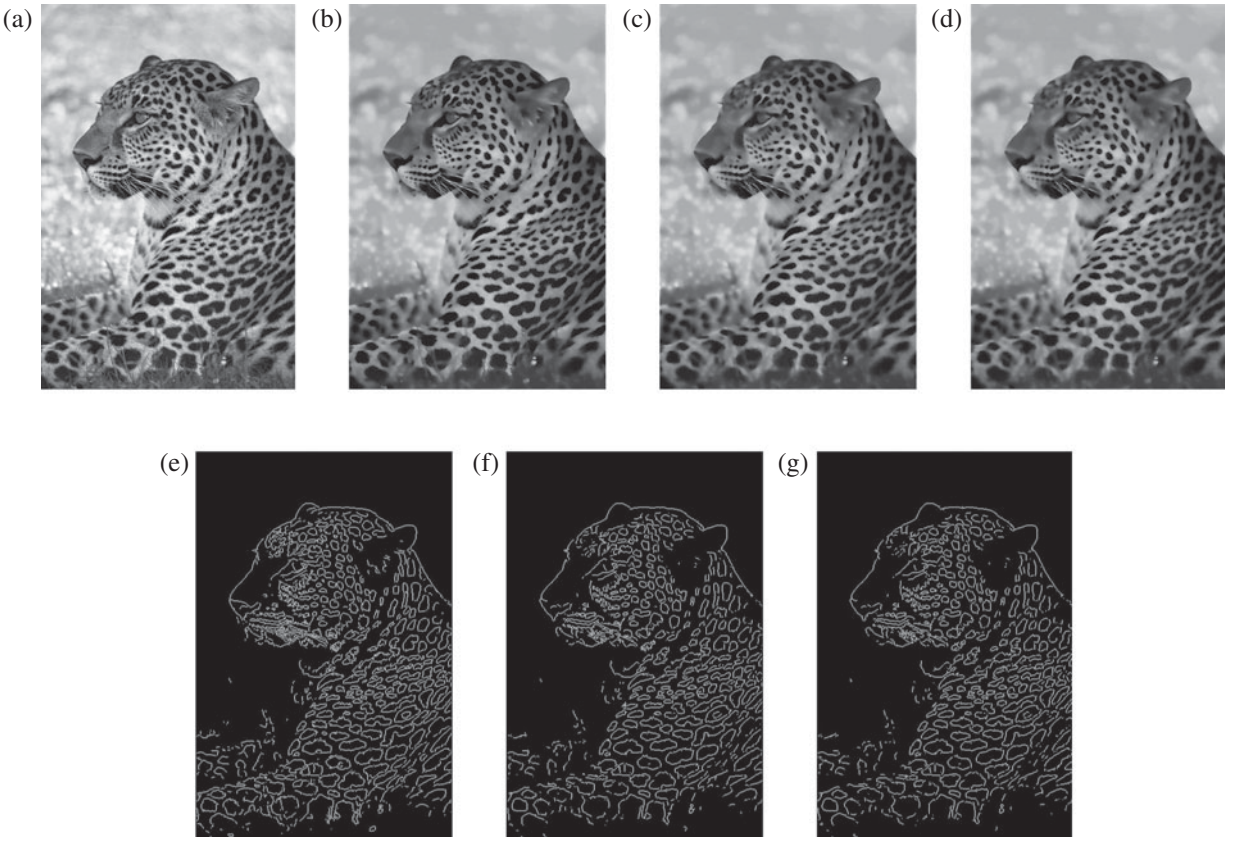

Figure 4. (a) Original panther image. (b)–(d) Smoothed versions of it by AD with thresholds $wep = 0.5$ and varying $sep \in \{0.01, 0.3, 0.4\}$ to fit the diffusion coefficient. (e)–(g) The respective edge images.

Table 2. Values for the least square fitting.

x	m_{21}	m_{31}
$C(x, y)$	sep	Wep

4. Experimental environment and obtained results

In this section, we use the AD equation of Perona–Malik with the proposed algorithm KMLS as an estimator of the contrast parameter to smooth the image, followed by a classical edge detector to obtain an edge image. The resulting edge images are compared with the results obtained using other smoothing algorithms. The aim is to show how the previous filtering of the image using the diffusion equation with our algorithm, greatly improves the subsequent edge images. Furthermore, we settle on the experimental environment based on an objective performance comparison of several edge detectors, in order to determine which one of those considered in the analysis obtains the best results.

4.1 Objective performance comparison method

Nowadays, it is well established in the literature that the visual inspection of the edge images obtained by several edge detectors cannot be the unique criterion to prove the superiority of one edge detector method with respect to the others. This is because each expert has different criteria and preferences and consequently, the reviews given by two experts can differ substantially. For this reason, the use of objective performance measures on edge detection is gaining popularity to compare the results obtained by different edge detection algorithms. There are several measures of performance for edge detection in the literature, see Lopez-Molina et al. (2013) and Papari and Petkov (2011). These measures require, in addition to the binary edge image with edges of one-pixel width (DE) obtained by the edge detector we want to evaluate, a reference edge image or *ground truth* edge image (GT) which is a binary edge image with edges of one-pixel width containing the real edges of the original image. That is, both images should satisfy the Canny criteria, forcing a representation of the edge images as binary images with edges of one-pixel width. In this work, we use the following quantitative performance error measures based on distance.

- An alternative formulation of *Pratt's figure of merit* ($PFoM^*$), defined as $PFoM^*(\mathrm{DE}, \mathrm{GT}) = 1 - PFoM(\mathrm{DE}, \mathrm{GT})$ where $PFoM(\mathrm{DE}, \mathrm{GT})$ is the

PFoM (Abdou and Pratt 1979)

$$PFoM(\mathrm{DE},\mathrm{GT}) = \frac{1}{\max\{|\mathrm{DE}|,|\mathrm{GT}|\}} \sum_{x\in\mathrm{DE}} \frac{1}{1+ad^2(x,\mathrm{GT})},$$

where $|\cdot|$ is the number of edge points in the image, $a \in \mathbb{R}^+$ is a scaling constant controlling the sensibility to the differences between DE and GT, generally fixed to 1/9 (Baddeley 1992) for keeping the values in [0,1], and d is the separation distance of an actual edge point to the ideal edge points (normally the Euclidean distance). This measure satisfies the property $PFoM^*(\mathrm{DE},\mathrm{GT}) = 0$ if and only if DT = GT, but it is not a symmetric error measure. A smallest value of $PFoM^*$ indicates a better capability to detect edges.

- The so-called *symmetric average distance* (SD_K) defined as

$$\mathrm{SD}_K(\mathrm{DE},\mathrm{GT}) = \frac{\left(\sum_{x\in\mathrm{DE}} d^K(x,\mathrm{GT}) + \sum_{x\in\mathrm{GT}} d^K(x,\mathrm{DE})\right)^{1/K}}{|\mathrm{DE}\cup\mathrm{GT}|^{1/K}}$$

where $K \in R^+$. This measure is a symmetric extension of the average distance with respect to the ground truth image, and also satisfies the property $D_K(\mathrm{DE},\mathrm{GT}) = 0$ if and only if DT = GT. When $K = 1$ or $K = 2$, we obtain the average symmetric surface distance or root mean square symmetric surface distance, respectively, as introduced by Heimann et al. (2009) for the comparison of segmented liver images.

These two measures are complementary since both have different properties. The *symmetric average distance* is sensitive to both false positives and false negatives, but it is less sensitive to the false negatives. It characterises the displacements of the edges in a reasonable way better than any other measure. The $PFoM^*$ measure performs differently with respect to the false positives, mainly because of the increase of $\max\{|\mathrm{DE}|,|\mathrm{GT}|\}$ when a false positive is added; it is not symmetric and it seems to be particularly sensitive to displacements. Recall that smoothing tends to displace the edges. Despite these, *PFoM* has been the most used quality measure in the literature, although some authors have made explicit the need for obtaining more accurate measurements (Peli and Malah 1982; Lopez-Molina et al. 2013).

Consequently, we need a database of images with their ground truth edge images in order to compare the outputs obtained by the different algorithms. Therefore, the images and their edge specifications from the public database of the University of South Florida[1] (Bowyer et al. 1999) have been used. In Bowyer et al. (1999), the details about the ground truth edge images and their use for the comparison of edge detectors are included. Furthermore, in order to increase the range of processed and treated images, and to verify the effectiveness of the proposed method, we also considered the Berkeley Segmentation Dataset[2] (BSD500) containing different outdoor scenes and object images together with its ground truth segmentation images (see Martin et al. 2001 and Arbelaez et al. 2011 for details). Because of this the two datasets are very different in their objectives, the first dataset is for evaluating edge detectors and the second one for evaluating segmentation algorithms, the results will be presented separately.

As previously mentioned in Section 3.1, the fixed combination of values, *sep* and *wep* that we use in the section of experimental results is $sep = 0.01$ and $wep = 0.5$. In Figures 5 and 6, we can see examples of the evolution of the objective performance measures as a function of the values of *wep* and *sep* for the Canny edge detector. Figure 5 shows, for the fixed value $sep = 0.01$, the Pratt and SD_K measures as a function of *wep* values, for 10 of the images in the database of the University of South Florida. As can be seen, for a fixed image, the variation of measures values is very soft and its differences for different values of *wep* are very small. The shape of the graphs of Pratt and SD_K measures in function of *wep* values, for a fixed value of *sep*, are very similar. Then, a convenient choice for a common value of *wep* for all the images and reaching a compromise between decreasing the measures and the conservation of some weak edges is $wep = 0.5$. However, in Figure 6 we show the objective performance measures as a function of the values of *sep*, for a fixed value $wep = 0.5$. Again, the variations in the values of the measures for the same image are very small. However, the value of $sep = 0.01$ provides the best value of the measure for 5 of the 10 images, then and taking into account the comments of Section 3.1, we set the value $sep = 0.01$.

4.2 *Obtained results and discussion*

Using the images from the public image database of Bowyer et al. (1999), three types of smoothing were carried out: Gaussian smoothing, AD smoothing using p-norm to estimate the contrast parameter k (Voci et al. 2004) and AD smoothing using the proposed algorithm KMLS to estimate k. After that, two classic edge detectors are applied to each smoothed image: the Canny and Prewitt edge detectors. The performance of our algorithm is first visually measured comparing the edge images obtained for each filtered image, and observing whether for each image from the database, the coupling AD + KMLS estimator

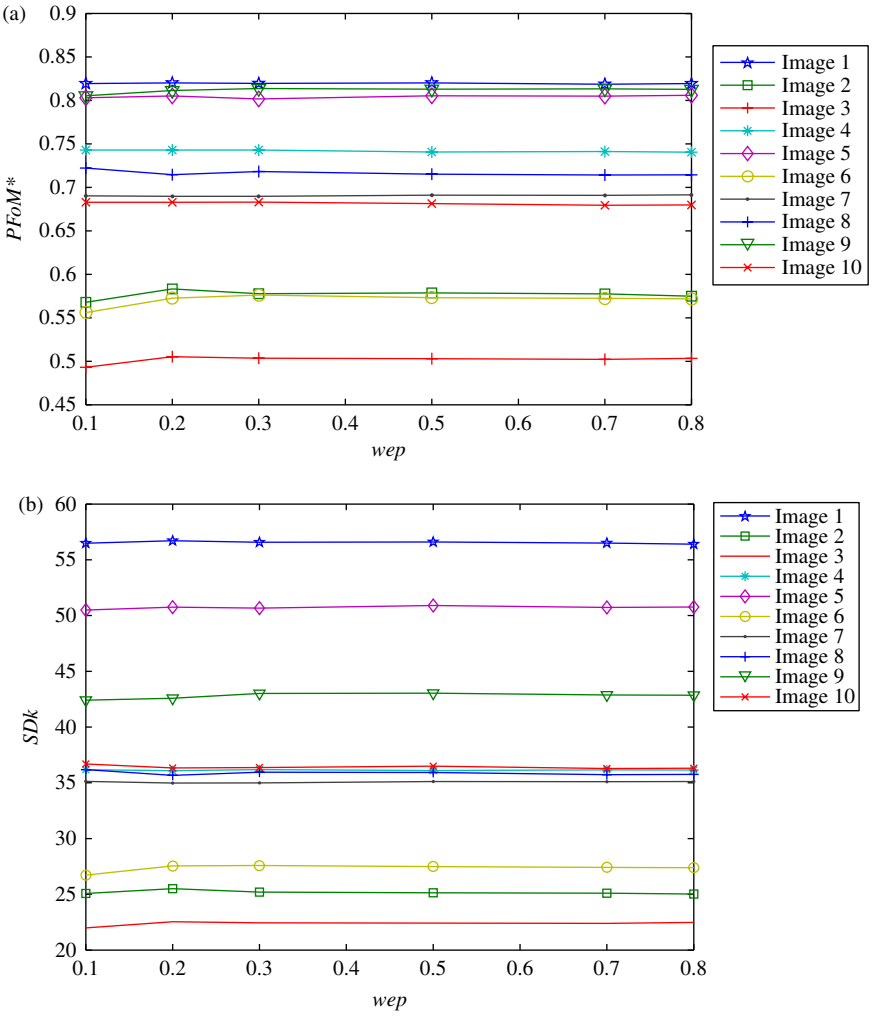

Figure 5. Evolution of the objective performance measures as a function of *wep* values, for a fixed value *sep* = 0.01 and the Canny edge detector. (a) $PFoM^*$ measure. (b) SD_K measure.

provides better results. To obtain a more objective evaluation of the quality of the obtained edge images, the objective performance measures described in Section 4.1 have been used.

Some results are shown in Figures 7–10; the first two figures show indoor scenes and the other two figures show outdoor scenes, one of them natural. As you can observe, the edge image were greatly improved when previously filtered by AD with KMLS. The coupling AD + KMLS provides edge images with a smaller number of edges, and therefore with smaller edges corresponding to irrelevant details and it is much closer to the ground truth image. This may be an indicator that the KMLS estimator performs better results than the other two methods. Visually the improvement is higher for the outdoor scenes, see Figures 9 and 10.

In Figures 11 and 12, we illustrate the behaviour of the objective performance error measures in the quality of the edge images obtained with the Canny algorithm. As mentioned earlier, we compare the quality of the edge images corresponding to three smoothing algorithms: in Figure 11, AD with KMLS versus AD with p-norm and in Figure 12, AD with KMLS versus Gaussian smoothing.

In Figures 11(a) and 12(a), the measure $PFoM^*$ with parameter equal to 1/9 is used. In this case using AD with KMLS filtering, the quality of the edge images was superior (that means smaller error measure) to AD with p-norm for 89.5% of the analysed images, but in the case of Gaussian smoothing (see Figure 12(a)) it was better for 81.25% of the analysed images. In Figures 11(b) and 12(b), the SD_K measure of parameter 2 is used. Considering the results of these two figures, we get a successful result for the edge images corresponding to our smoothing algorithm for 56.25% of the analysed images. With regard to AD with p-norm smoothing, it was better for 66.6% and 64.3% with respect to Gaussian filtering of the analysed images.

The proposed method achieved better results for most of the images in terms of all two quality measures but the

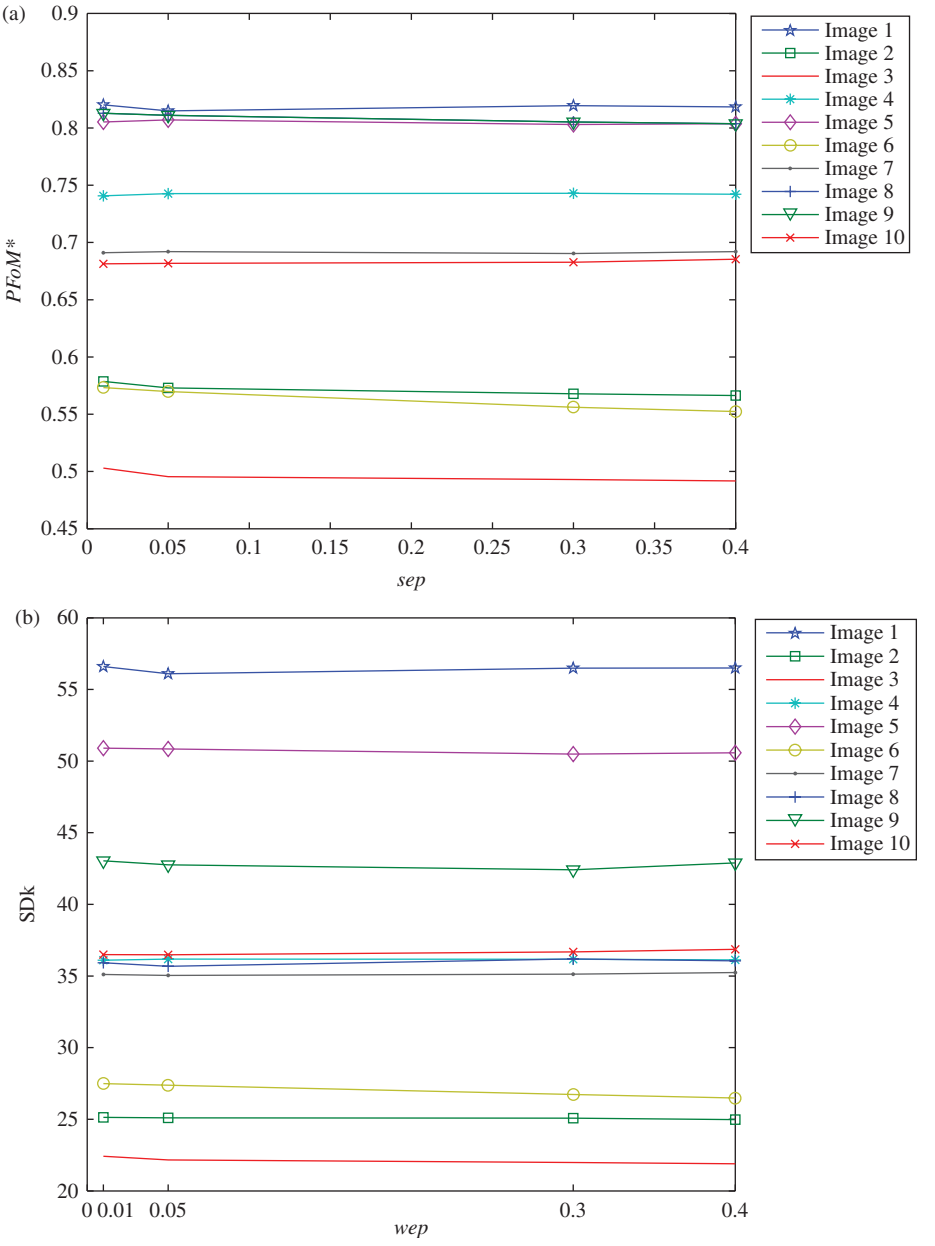

Figure 6. Evolution of the objective performance measures as a function of *sep* values, for a fixed value $wep = 0.5$ and the Canny edge detector. (a) $PFoM^*$ measure. (b) SD_K measure.

measure $PFoM^*$ gives better results than the measure SD_K. For the images where our algorithm did not give better results, we corroborate that as the quality of the smoothing is not measured directly, but through the detection of edges, the thresholds used for those methods to classify the pixels as edges or not, penalise a bit the smoothing with KMLS.

Considering the edge images obtained by the edge detector algorithm of Prewitt, a similar experiment is carried out and similar results were obtained. In Figures 13 and 14, we show the graphs for the objective error measures. In this case, if we apply our algorithm as mentioned before we also get better results for most of the images in terms of all two quality measures. However, the percent of images where our algorithm works better is smaller compared with the edge images obtained by Canny. Using the measure $PFoM^*$, we have obtained with our algorithm a superior quality of 52% of the analysed images against 39.5% for the Gaussian smoothing and 8.33% for AD with p-norm (see Figures 13(a) and 14(a)). Using the measure SD_K, the proposed algorithm gives us better results of 62.5% of the analysed images against 29.1% for AD with p-norm and 8.3% for Gaussian smoothing (see Figures 13(b) and 14(b)). As you can see,

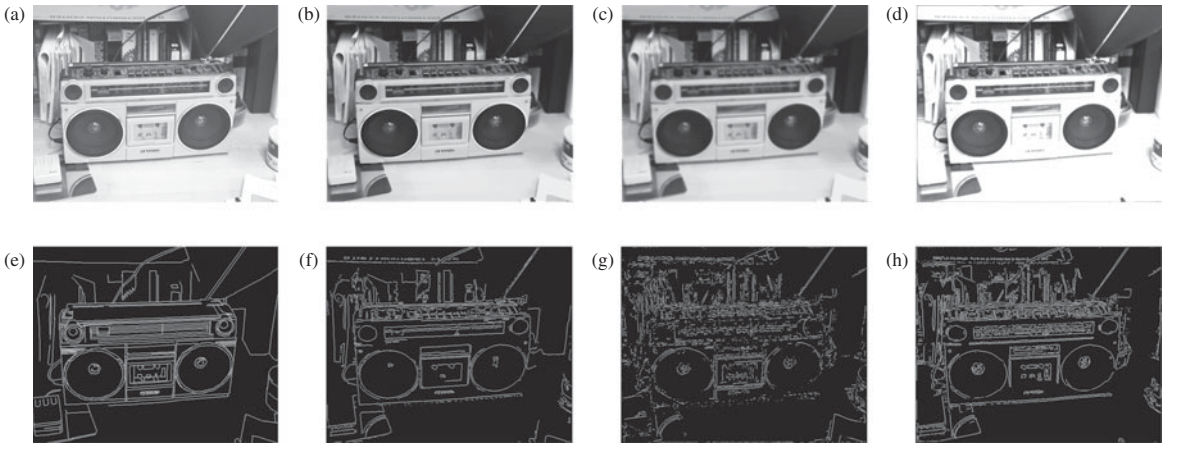

Figure 7. (a) Original recording image. (b) A smoothed version of the image by AD with k taken according to KMLS. (c) A smoothed version using AD with k taken according to p-norm. (d) Gaussian smoothing. (e) Ground truth edge image. (f)–(h) Edge images using Canny edge detector for (b)–(d), respectively.

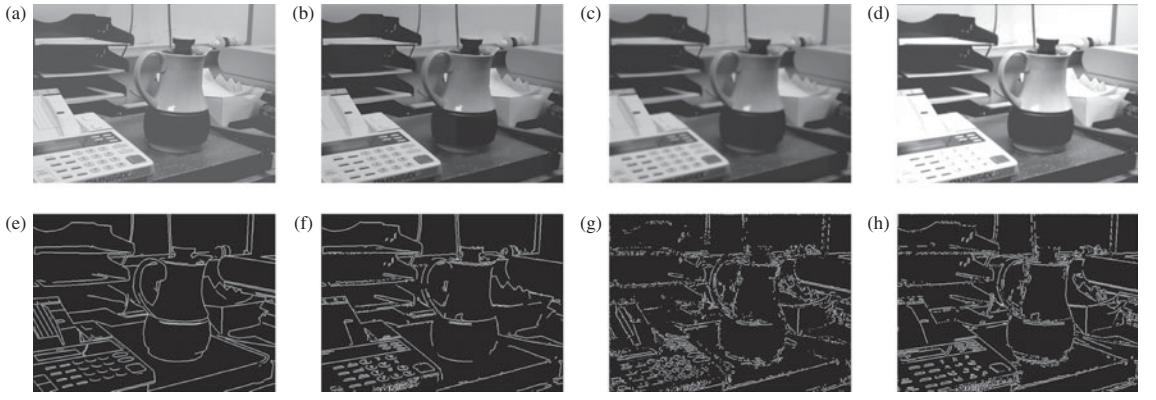

Figure 8. (a) Original water heater image. (b) A smoothed version of the image by AD with k taken according to KMLS. (c) A smoothed version using AD with k taken according to p-norm. (d) Gaussian smoothing. (e) Ground truth edge image. (f)–(h) Edge images using Canny edge detector for (b)–(d), respectively.

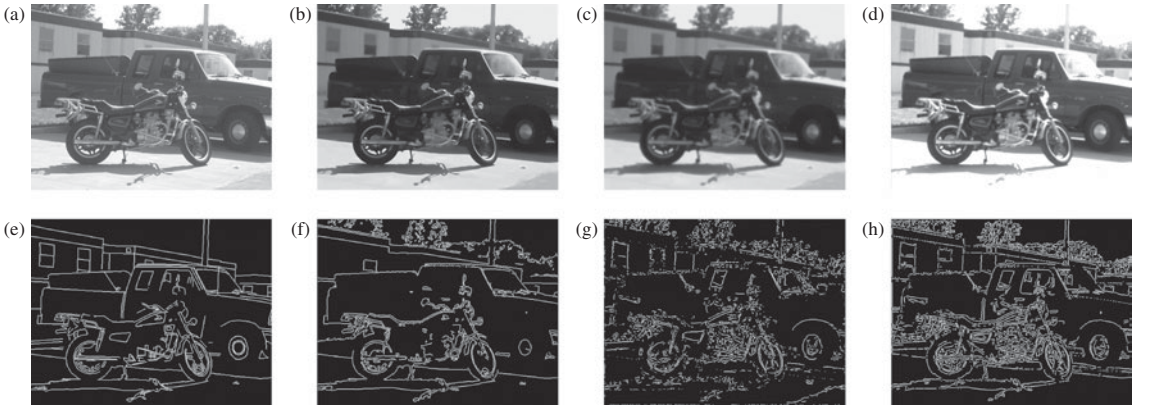

Figure 9. (a) Original outdoor image. (b) Smoothed image by AD with k taken according to KMLS. (c) Smoothed image by AD with k taken according to p-norm. (d) Gaussian smoothing. (e) Ground truth edge image. (f)–(h) Edge images using Canny edge detector for (b)–(d), respectively.

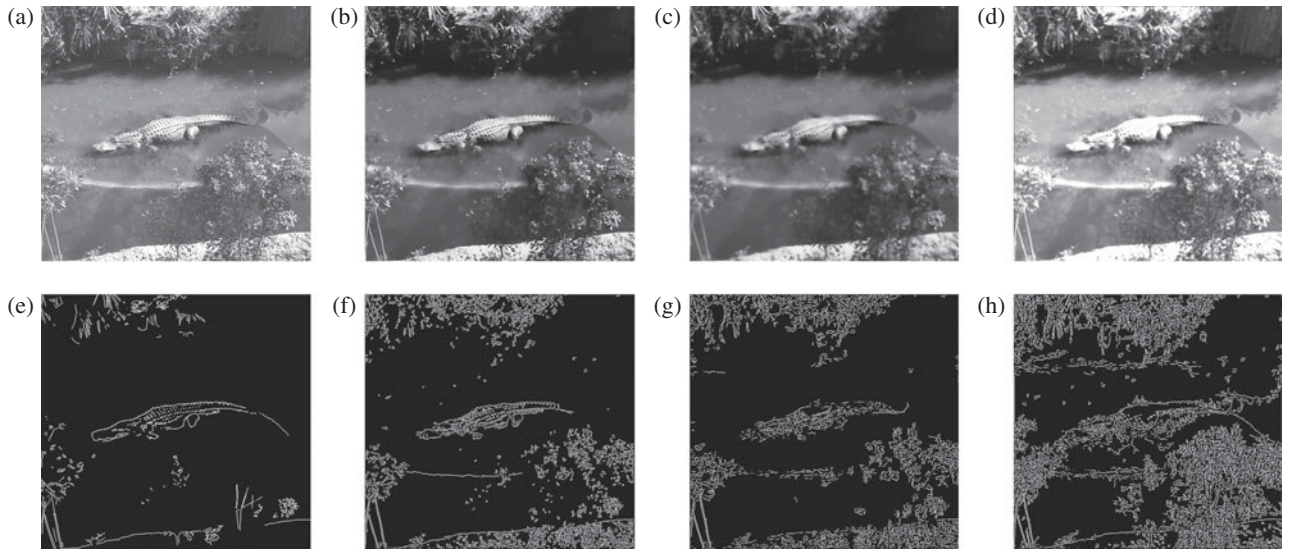

Figure 10. (a) Original natural image of a crocodile. (b) A smoothed version of it by AD with k taken according to KMLS. (c) A smoothed version off it by AD with k taken according to p-norm. (d) Gaussian smoothing. (e) Ground truth edge image. (f)–(h) Edge images using Canny edge detector for (b)–(d), respectively.

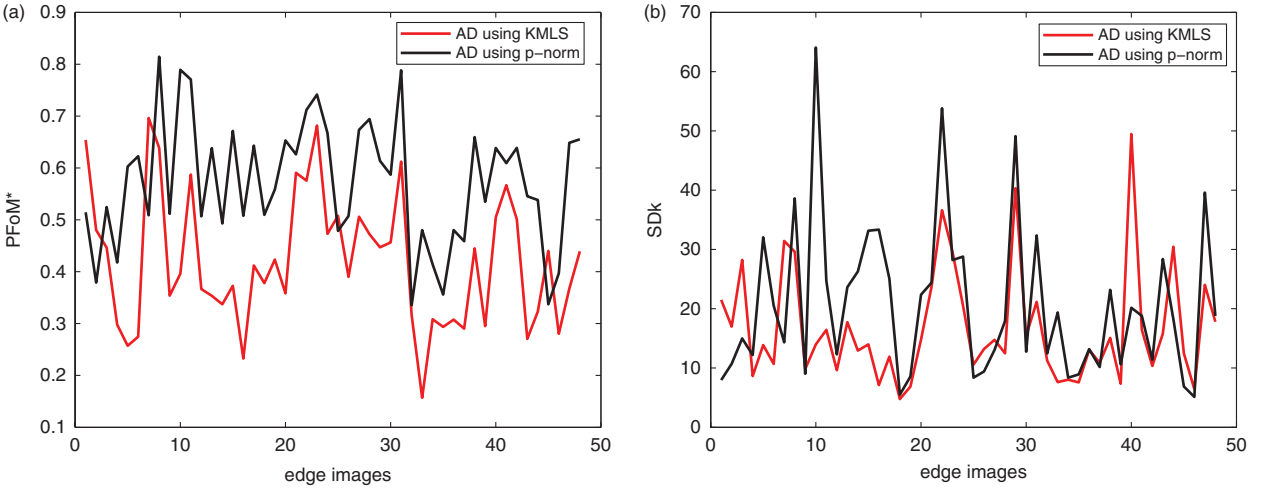

Figure 11. Comparison of the error measure for the Canny edge detector in case of preprocessing by AD with KMLS versus AD with p-norm. (a) Objective performance measure $PFoM^*$ (parameter 1/9). (b) Objective performance measure SD_K (parameter 2). (Colour online.)

for Prewitt edge detector, the SD_K measure gives better results as much for our algorithm as for that of the p-norm. It is the opposite with the edge detector of Canny. This could be considered normal, since both classical edge detectors are very different and, as noted in Section 4.1, the two measures have complementary behaviours.

A second similar set of experiments was carried out on a subset of images of the BSD500 dataset. The results are shown in Figures 15 and 16. Figure 15 shows the results for the Canny edge detector and Figure 16 for Prewitt edge detector. Both show the results using AD with KMLS versus Gaussian filtering. In the case of Canny edge detector and the measure $PFoM^*$, the quality of the edge images using AD with KMLS was superior to the Gaussian filtering for 83% of the analysed images; but in the case of the SD_K measure this percentage increases to 87%. Considering the edge images obtained using the Prewitt edge detector, if we apply our algorithm (AD whit KMLS) we also obtain better results for most of the images in terms of the two quality measures, but the percentage of images where our algorithm performs better than the Gaussian filtering is 64% for both measures, percentage that is slightly higher than that obtained with the other database. Note that this behaviour, in relation to the

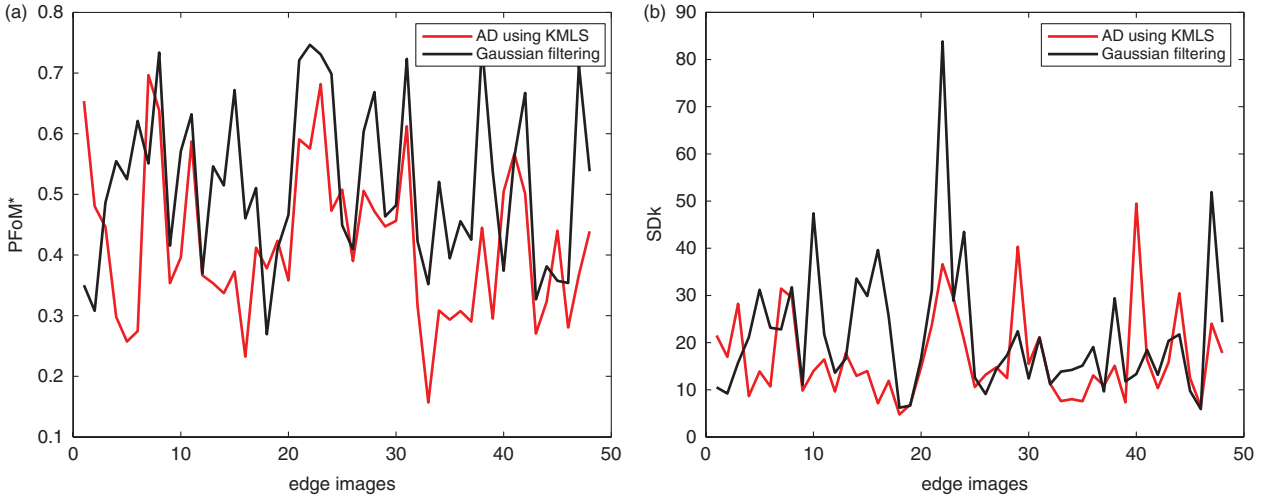

Figure 12. Comparison of the error measure for the Canny edge detector in case of preprocessing by AD with KMLS versus Gaussian smoothing. (a) Objective performance measure $PFoM^*$ (parameter 1/9). (b) Objective performance measure SD_K (parameter 2). (Colour online.)

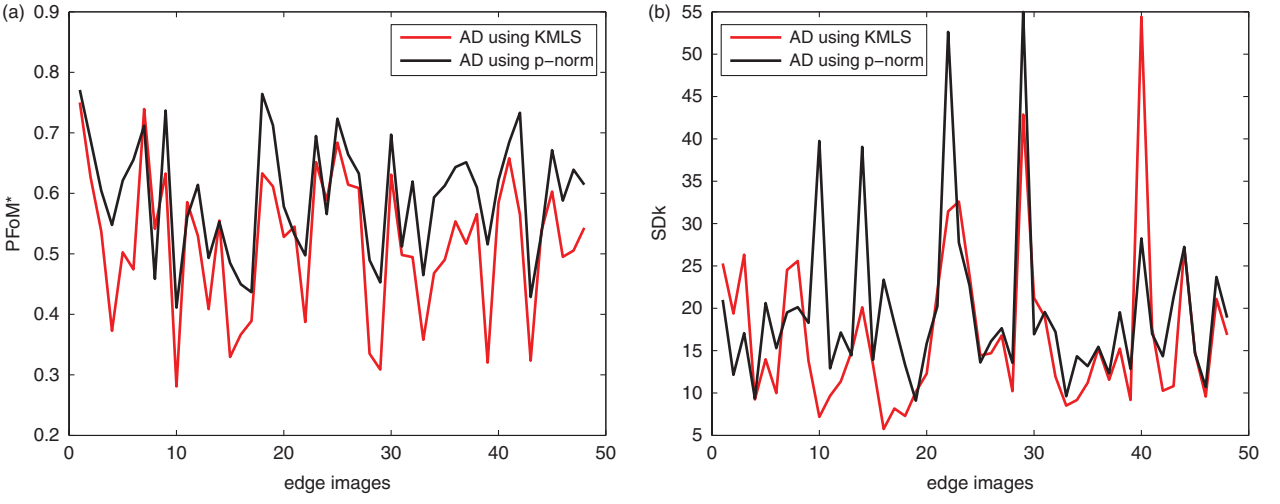

Figure 13. Comparison of the error measure for Prewitt edge detector in case of preprocessing by AD with KMLS versus AD with p-norm. (a) $PFoM^*$ (parameter 1/9) measure. (b) SD_K (parameter 2) measure. (Colour online.)

comparison of AD using KMLS with the Gaussian filter is similar to that obtained with the database of University of South Florida. A similar behaviour has been observed in relation to the comparison of the quality of edge images obtained with both edge detectors after smoothing with AD using KMLS versus AD using p-norm.

5. Conclusions

In this contribution, a novel estimation methodology to obtain the contrast parameter in the Perona–Malik AD filter is presented. The methodology is based on a partition of the pixel set of the image, according to its gradient magnitude and combined with a least square fitting for the diffusion coefficient. At each integration step, a new contrast parameter is obtained. The most remarkable characteristic of the estimation is its independence of the experimental test. The obtained edge images in every case were evaluated using the $PFoM^*(1/9)$ and the SD_K (2) objective performance error measures. The proposed method achieved better results for most of the images in terms of both quality measures, but the best results are reached by Canny edge detector using the $PFoM^*(1/9)$ measure. This is an indicator that using the KMLS estimator filtering provides better results than the other two methods.

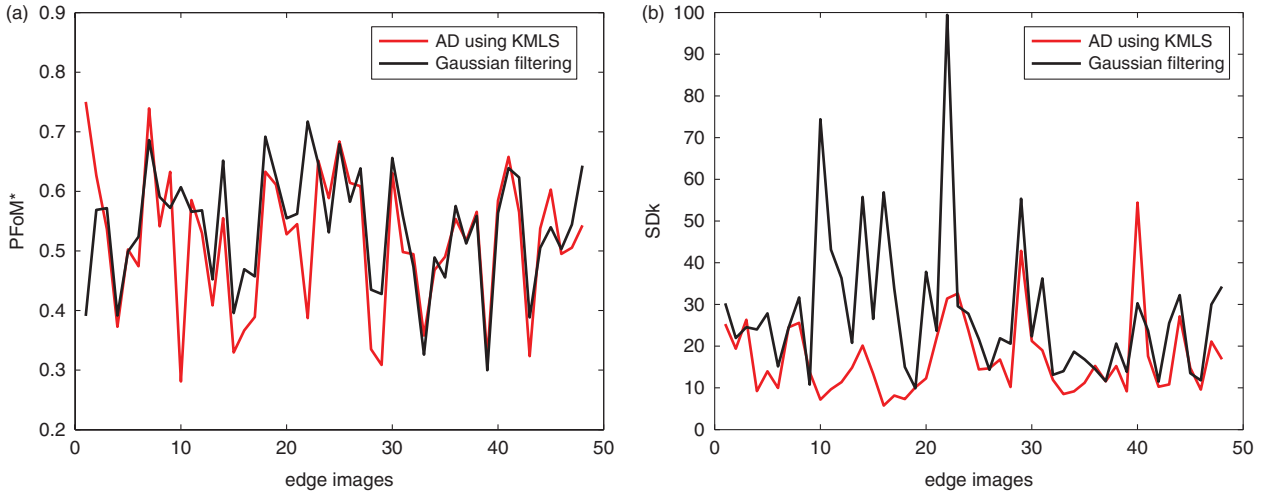

Figure 14. Comparison of the error measure for Prewitt edge detector in case of preprocessing by AD with KMLS versus Gaussian filtering. (a) $PFoM^*$ (parameter 1/9) measure. (b) SD_K (parameter 2) measure.

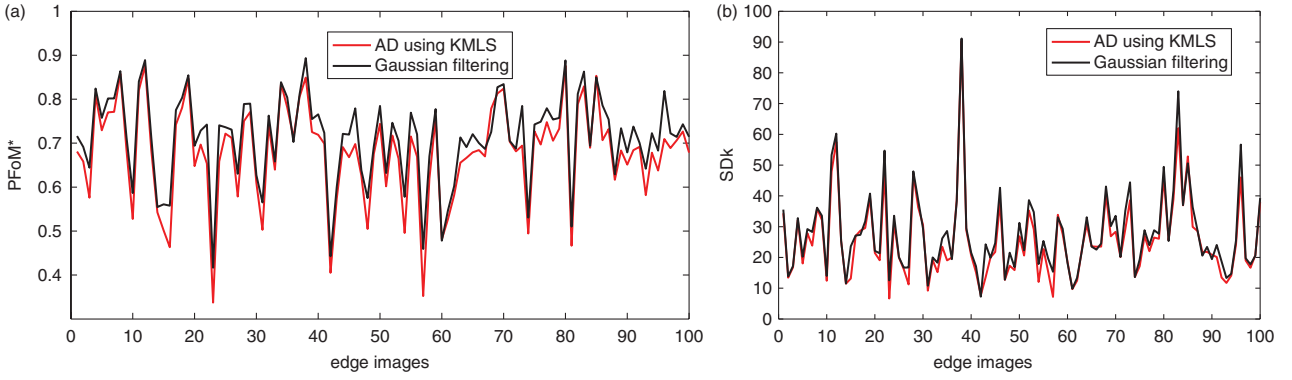

Figure 15. Comparison of the error measure for the images of the BSD500 dataset and the Canny edge detector in case of preprocessing by AD with KMLS versus Gaussian filtering. (a) $PFoM^*$ (parameter 1/9) measure. (b) SD_K (parameter 2) measure.

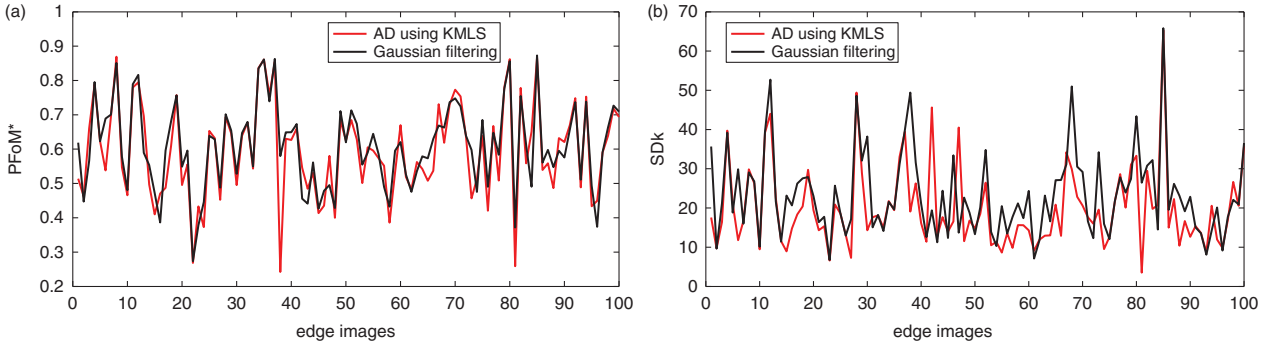

Figure 16. Comparison of the error measure for the images of the BSD500 dataset and the Prewitt edge detector in case of preprocessing by AD with KMLS versus Gaussian filtering. (a) $PFoM^*$ (parameter 1/9) measure. (b) SD_K (parameter 2) measure. (Colour online.)

The 'Partition and Adjustment' methodology leaves open a whole field of research and experimentation, because it is possible to use different clustering methods for partitioning the set of pixels of an image, and different types of curve fits changing the norm for approximation. All this leads to the development of new estimators that undoubtedly are very necessary for achieving good results in edge detection and image segmentation.

Funding

This work was partially supported by the Government Spanish MAEC-AECID A2/037538/11 project, and the Government Spanish Grant [grant number MTM2009-10320] with FEDER support.

Notes

1. This image dataset can be downloaded from ftp://figment.csee.usf.edu/pub/ROC/edge_comparison_dataset.tar.gz.
2. This image dataset can be downloaded from http://www.eecs.berkeley.edu/Research/Projects/CS/vision/bsds/.

References

Abdou I, Pratt W. 1979. Quantitative design and evaluation of enhancement/thresholding edge detectors. Proc IEEE. 67(5):753–763.

Alvarez L, Lions PL, Morel JM. 1992. Image selective smoothing and edge detection by non-linear diffusion. ii. SIAM J Numer Anal. 29(3):845–866.

Arbelaez P, Maire M, Fowlkes C, Malik J. 2011. Contour detection and hierarchical image segmentation. IEEE Trans Pattern Anal Mach Intell. 33(5):898–916.

Baddeley AJ. 1992. Errors in binary images and an LP version of the Hausdorff metric. Nieuw Arch Wiskunde. 10:157–183.

Bankman IN, ed. 2008. Handbook of medical image processing and analysis. 2nd ed. Burlington (MA): Academic Press.

Barash D, Kimmel R. 2000. An accurate operator splitting scheme for non-linear diffusion filtering (HP Laboratories technical report). Haifa: Hewlett-Packard Laboratories.

Black M, Sapiro G, Marimont D, Heeger D. 1998. Robust anisotropic diffusion. IEEE Trans Image Process. 7(3):421–432.

Bovik AC. 2009. The essential guide to image processing. Burlington (MA): Academic Press.

Bowyer K, Kranenburg C, Dougherty S. 1999. Edge detector evaluation using empirical ROC curves. Comput Vision Pattern Recogn. 1:354–359.

Canny J. 1986. A computational approach to edge detection. IEEE Trans Pattern Anal Mach Intell. 8(6):679–698.

Catté F, Lions PL, Morel JM, Coll T. 1992. Image selective smoothing and edge detection by non-linear diffusion. SIAM J Numer Anal. 29(1):182–193.

Chai H, Wee L, Supriyanto E. 2011. Ultrasound images edge detection using anisotropic diffusion in canny edge detector framework. WSEAS Trans Biol Biomed. 8(2):51–60.

Chan T, Shen J. 2005. Image processing and analysis: variational, PDE, wavelet, and stochastic methods. Philadelphia (PA): Society for Industrial and Applied Mathematics (SIAM).

Chan TF, Shen JJ, Vese L. 2003. Variational PDE models in image processing. Not Am Math Soc. 50(1):14–26.

Charbonnier P, Blanc-Feraud L, Aubert G, Barlaud M. 1997. Deterministic edge-preserving regularization in computed imaging. IEEE Trans Image Process. 6(2):298–311.

Chen D, MacLachlan S, Kilmer M. 2011. Iterative parameter-choice and multigrid methods for anisotropic diffusion denoising. SIAM J Sci Comput. 33(5):2972–2994.

Duarte-Carvajalino JM, Castillo PE, Velez-Reyes M. 2007. Comparative study of semi-implicit schemes for non-linear diffusion in hyperspectral imagery. IEEE Trans Image Process. 16(5):1303–1314.

Duda RO, Hart PE, Stork DG. 2001. Pattern classification. 2nd ed. New York (NY): Wiley-Interscience.

Gilboa G, Sochen N, Zeevi YY. 2002. Forward-and-backward diffusion processes for adaptive image enhancement and denoising. IEEE Trans Image Process. 11(7):689–703.

Heimann T, Van Ginneken B, Styner M, Arzhaeva Y, Aurich V, Bauer C, Beck A, Becker C, Beichel R, Bekes G. 2009. Comparison and evaluation of methods for liver segmentation from CT datasets. IEEE Trans Med Imaging. 28(8):1251–1265.

Kaur J, Mikula K. 1995. Solution of non-linear diffusion appearing in image smoothing and edge detection. Appl Numer Math. 17(1):47–59.

Koenderink JJ. 1984. The structure of images. Biol Cybern. 50(5):363–370.

Lopez-Molina C, De Baets B, Bustince H. 2013. Quantitative error measures for edge detection. Pattern Recogn. 46(4):1125–1139.

Mallat S. 2008. A wavelet tour of signal processing: the sparse way. 3rd ed. Burlington (MA): Academic Press.

Martin D, Fowlkes C, Tal D, Malik J. 2001. A database of human segmented natural images and its application to evaluating segmentation algorithms and measuring ecological statistics. In: Proceedings of the 8th international conference computer vision. Vol. 2. p. 416–423.

Mendrik A, Vonken EJ, Rutten A, Viergever M, Van Ginneken B. 2009. Noise reduction in computed tomography scans using 3-D anisotropic hybrid diffusion with continuous switch. IEEE Trans Med Imaging. 28(10):1585–1594.

Papari G, Petkov N. 2011. Edge and line oriented contour detection: state of the art. Image Vision Comput. 29(2–3):79–103.

Peli T, Malah D. 1982. A study of edge detection algorithms. Comput Graphics Image Process. 20(1):1–21.

Perona P, Malik J. 1990. Scale-space and edge detection using anisotropic diffusion. IEEE Trans Pattern Anal Mach Intell. 12(7):629–639.

Stoer J, Bulirsch R. 1993. Introduction to numerical analysis. 2nd ed. New York (NY): Springer-Verlag.

Tsiotsios C, Petrou M. 2013. On the choice of the parameters for anisotropic diffusion in image processing. Pattern Recogn. 46(5):1369–1381.

Voci F, Eiho S, Sugimoto N, Sekibuchi H. 2004. Estimating the gradient in the Perona–Malik equation. IEEE Signal Process Mag. 21(3):39–65.

Weeratunga SK, Kamath C. 2003. Comparison of PDE-based non-linear anistropic diffusion techniques for image denoising. Proc. of SPIE, Image Processing: Algorithms and Systems II. 5014:201–212. doi: 10.1117/12.477744.

Weickert J. 1998. Anisotropic diffusion in image processing. ECMI Series. Stuttgart: Teubner.

Weickert J. 1999. Coherence-enhancing diffusion filtering. Int J Comput Vision. 31(2-3):111–127.

Weickert J, Romeny B, Viergever M. 1998. Efficient and reliable schemes for non-linear diffusion filtering. IEEE Trans Image Process. 7(3):398–410.

Witkin AP. 1983. Scale-space filtering. In: Proceedings of the 8th international joint conference on artificial intelligence; Karlsruhe, West Germany. Vol. 2. San Francisco, CA: Morgan Kaufmann; p. 1019–1022.

Zhang Y, Yang X. 2010. On the acceleration of AOS schemes for non-linear diffusion filtering. J Multimedia. 5(6):605–612.